Critical Examination of Two-Equation Turbulence Closure Models for Boundary Layers

Thomas L. Chambers* and David C. Wilcox†
DCW Industries, Inc., Studio City, Calif.

An objective three-part comparison of the Jones-Launder, Ng-Spalding, Saffman-Wilcox, and Wilcox-Traci two-equation turbulence models has been conducted. First, a term-by-term algebraic comparison demonstrated that the forms of the model equations appear very similar for the four models. However, the comparison also indicated that the Saffman-Wilcox and Wilcox-Traci dissipation-rate formulations admit straightforward integration through the viscous sublayer, whereas integration through the viscous sublayer is a more difficult issue with the Jones-Launder dissipation-function and the Ng-Spalding length-scale formulations. Next, numerical computations were conducted in which the models were applied to four equilibrium boundary-layer flows including adverse, zero, and favorable pressure gradients. The models were tested using the same numerics, boundary conditions, and starting profiles. Overall, the Ng-Spalding and Wilcox-Traci models yielded results in closest agreement with experimental data. Most importantly, these two models are as accurate as mixing length for equilibrium boundary layers. Computations of zero pressure gradient flow over a convex wall composed the final part of the comparison. With rationally devised streamline curvature modifications, the Jones-Launder, Ng-Spalding, and Wilcox-Traci models yielded excellent agreement with experimental data for the flow considered.

I. Introduction

SINCE most interesting fluid mechanical problems involve turbulence, researchers have directed a great deal of effort at finding reliable predictive methods for turbulent flowfields. A recent outgrowth of this research has been the development of second-order-closure two-equation turbulence models, i.e., models which utilize two parameters to characterize the turbulence and to determine the eddy diffusivity, with each parameter satisfying a nonlinear diffusion equation. Such models have proliferated,[1-8] and each is supposedly universally applicable to turbulent fluid flows. A great deal of success has been obtained for a wide variety of flows including effects which cannot be accurately analyzed with conventional mixing-length approaches such as boundary-layer separation[9] and transition.[10]

As first noted by Wilcox and Alber,[3] two-equation models bear a great deal of similarity. While previous comparisons of two-equation models have been made,[11,12] no one has made more than a cursory examination. In particular, no one has presented parallel numerical solautions for the various models.

The purpose of this study has been to establish model differences and similarities, and to determine precisely how well two-equation theories perform relative to each other. Four models have been considered, viz, those developed by Jones and Launder,[5] Ng and Spalding,[6] Saffman and Wilcox,[2,7] and Wilcox and Traci.[8] There is no need to consider additional models as all current two-equation models are variants of these four.

In Sec. II, the model equations are cast in forms similar to the Wilcox-Traci model, and compared systematically; viscous modifications needed to allow integration through the sublayer are discussed. Sec. III presents results of numerical computations for four equilibrium boundary layers; comparisons with experimental data are included. Applicability of the models to turbulent flows with curved streamlines is assessed in Sec. IV; curvature modifications are devised for each model. The final section summarizes results and conclusions.

Presented as Paper 76-352 at the AIAA 9th Fluid and Plasma Dynamics Conference, San Diego, Calif., July 14-16, 1976; submitted Sept. 27, 1976; revision received March 22, 1977.

Index category: Boundary Layers and Convective Heat Transfer—Turbulent.

*Associate Engineer.

†President. Associate Fellow AIAA.

II. Term-by-Term Comparisons

Throughout the paper, the incompressible forms (i.e., negligible Mach number) of the equations are considered. In the numerical comparisons, the incompressible forms are further restricted to the inviscid equations (negligible molecular viscosity-high Reynolds number) due to the nonuniversality in the way viscous effects are included in the various turbulence models. Therefore, none of the models receive preferential treatment when their computational accuracy is assessed. The incompressible, high Reynolds number versions of the equations are also the focal point of the term-by-term comparisons. However, it is very instructive as well to analyze the models when molecular viscosity is added to the diffusion terms, as done by Saffman and Wilcox[7] and later by Wilcox and Traci[8] when developing viscous modifications for their respective models. Hence, the character of the viscous equations near a solid boundary is also considered in this section.

For all models, the conservation of mass and momentum equations appropriate for boundary layers are identical. Hence, turning our attention just to the high Reynolds number forms, the aforementioned equations are as follows:

$$\partial u/\partial x + \partial v/\partial y = 0 \tag{1}$$

$$\mathrm{d}u/\mathrm{d}t = -1/\rho \mathrm{d}p/\mathrm{d}x + \partial[\epsilon \partial u/\partial y]/\partial y \tag{2}$$

where u and v are velocity components in the streamwise, x, and surface-normal, y, directions, respectively; t is time and $\mathrm{d}/\mathrm{d}t = \partial/\partial t + u \cdot \nabla$; p and ρ denote pressure and density; and ϵ is the eddy diffusivity.

Commonly, two-equation models employ a turbulent mixing energy, e, as one of the parameters. The second parameter used by different turbulence researchers is either dissipation function, ϵ_d, length scale, ℓ, or dissipation rate, ω. Of the numerous models available for comparison, we select the Jones-Launder $e-\epsilon_d$ model, the Ng-Spalding $e-\ell$ model, the Saffman-Wilcox $e-\omega$ model, and the Wilcox-Traci $e-\omega$

model; the respective transport equations are as follows:

Jones-Launder Dissipation-Function Model

$$de/dt = \epsilon\{\partial u/\partial y\}^2 - \epsilon_d + \partial\{(\epsilon/\sigma_e)\partial e/\partial y\}/\partial y \quad (3)$$

$$d\epsilon_d/dt = c_1(\epsilon_d/e)\epsilon\{\partial u/\partial y\}^2 - c_2\epsilon_d{}^2/e + \partial\{(\epsilon/\sigma_\epsilon)\partial\epsilon_d\}\partial\epsilon_d/\partial y\}/\partial y \quad (4)$$

$$\epsilon = c_\mu e^2/\epsilon_d \quad (5)$$

$$c_1 = 1.55, \quad c_2 = 2, \quad c_\mu = .09, \quad \sigma_e = 1, \quad \sigma_\epsilon = 1.3 \quad (6)$$

Ng-Spalding Length-Scale Model

$$de/dt = \epsilon\{\partial u/\partial y\}^2 - c_D e^{3/2}/\ell + \partial\{(\epsilon/\sigma_e)\partial e/\partial y\}/\partial y \quad (7)$$

$$d(e\ell)/dt = c_p\ell\epsilon\{\partial u/\partial y\}^2 - [c_m + c_w\{\ell/y\}^6]e^{3/2} + \partial\{(\epsilon/\sigma_z)\partial/\partial y(e\ell)\}/\partial y \quad (8)$$

$$\epsilon = e^{1/2}\ell \quad (9)$$

$$c_D = .09, \quad c_p = .98, \quad c_m = .059, \quad c_w = 702, \quad \sigma_e = \sigma_z = 1 \quad (10)$$

Saffman-Wilcox Dissipation-Rate Model

$$de/dt = \alpha^*|\partial u/\partial y|e - \beta^*\omega e + \partial\{\sigma^*\epsilon\partial e/\partial y\}/\partial y \quad (11)$$

$$d\omega^2/dt = \alpha|\partial u/\partial y|\omega^2 - \beta\omega^3 + \partial\{\sigma\epsilon\partial\omega^2/\partial y\}/\partial y \quad (12)$$

$$\epsilon = e/\omega \quad (13)$$

$$\alpha^* = 3/10, \quad \beta^* = .09, \quad \sigma^* = \sigma = 1/2,$$

$$\alpha = \alpha^*[\beta/\beta^* - 4\sigma\kappa^2/\alpha^*], \quad 5/3 < \beta/\beta^* < 2 \quad (14)$$

Wilcox-Traci Dissipation-Rate Model

$$de/dt = \alpha^*|\partial u/\partial y|e - \beta^*\omega e + \partial[\sigma^*\epsilon\partial e/\partial y]/\partial y \quad (15)$$

$$d\omega^2/dt = \alpha|\partial u/\partial y|\omega^2 - \{\beta + 2\sigma[\partial(e^{1/2}/\omega)/\partial y]^2\}\omega^3 + \partial[\sigma\epsilon\,\partial\omega^2/\partial y]/\partial y \quad (16)$$

$$\epsilon = e/\omega \quad (17)$$

$$\alpha^* = 3/10, \quad \beta^* = .09, \quad \sigma^* = \sigma = 1/2, \quad \beta = .15, \quad \alpha = 1/3 \quad (18)$$

In Eq. (14), the quantity κ is Karman's constant.

All four models use a turbulent mixing energy equation. Commonly, e is assumed to be the turbulent kinetic energy. However, Wilcox and Chambers[13] have shown that, more appropriately, e should be interpreted as $9/4 < v'^2 >$ where v' is the fluctuating component of the velocity normal to the surface and $< >$ denotes time average. The ramifications of this intepretation of e will be seen in subsequent sections. The second turbulence parameter differs for the four models. However, by following the arguments of Wilcox and Alber,[3] all of the models can be cast in a "canonical" form, thus facilitating comparison of the models.

Table 1 Terms in transformed model equations

Model	P	Φ
Jones-Launder	$\epsilon(\partial u/\partial y)^2$	$2(\sigma-\sigma^*)(\omega^2/e)\partial(\epsilon\partial e/\partial y)/\partial y + 2\sigma\partial\omega/\partial y\,\partial e/\partial y + \frac{1}{2}\sigma(\omega/e)(\partial e/\partial y)^2$
Ng-Spalding	$\epsilon(\partial u/\partial y)^2$	$2c_w(\ell/y)^6\omega^3$
Saffman-Wilcox	$\alpha^* e\|\partial u/\partial y\|$	0
Wilcox-Traci	$\alpha^* e\|\partial u/\partial y\|$	0

Canonical Forms

The eddy viscosity, ϵ, is used in the same manner in each model as an integral part of approximating the Reynolds shear stress. The various expressions for ϵ can be equated and the following relations between ϵ_d, ω, and ℓ are established.

$$\epsilon_d = c_\mu e\omega, \quad \ell = e^{1/2}/\omega \quad (19)$$

Using the change of variables defined in Eq. (19), the four models can be transformed into the following "canonical form.

$$de/dt = \underbrace{P}_{①} \underbrace{-\beta^*\omega^3}_{②} + \underbrace{\partial[\sigma^*\epsilon\partial e/\partial y]/\partial y}_{③} \quad (20)$$

$$d\omega^2/dt = \underbrace{c_\omega(\omega^2/e)P}_{①} \underbrace{-\beta\omega^3}_{②} + \underbrace{\partial[\sigma\epsilon\,\partial\omega^2/\partial y]/\partial y}_{③} \underbrace{-\chi\sigma(\partial\ell/\partial y)^2\omega^3}_{④} + \underbrace{\Phi}_{⑤} \quad (21)$$

Terms in Eqs. (20) and (21) numbered ①, ②, and ③ are referred to as production, dissipation, and diffusion, respectively; term ④ is referred to as gradient dissipation while ⑤ represents other terms not falling in categories ①-④. The terms P and Φ appearing in the transformed equations are tabulated in Table 1; values of the constants β, β^*, etc., are given in Table 2. Differences between the field equations fall into three categories, namely, differences in production terms, gradient dissipation terms, and other subtle differences. First, the Saffman-Wilcox and Wilcox-Traci production terms are linear in $\partial u/\partial y$ while the Jones-Launder and Ng-Spalding production terms are proportional to $(\partial u/\partial y)^2$. Second, with the exception of the Saffman-Wilcox model, each model has a gradient dissipation term; the value of χ is larger for the Ng-Spalding model than for the other models. Finally, the Ng-Spalding model has an additional "wall-dissipation" term which resembles the gradient dissipation term; its effect would be to decrease the effective value of χ. Also, the Jones-Launder model has a turbulent-energy diffusion term in the ω^2 equation because of their assumption that $\sigma \neq \sigma^*$.

Values of the coefficients, c_ω, β, and β^* differ only slightly from model to model (Table 2). However, values for σ and σ^* used in the Saffman-Wilcox and Wilcox-Traci models are smaller than values used in the other models.

Wilcox and Chambers[13] have shown that, in calculations with the Saffman model, results are relatively insensitive to the precise form of the production terms. For equilibrium boundary layers, computed flow properties using $P = \alpha^* e|\partial u/\partial y|$ differ from corresponding properties computed with $P = \epsilon(\partial u/\partial y)^2$ by less than 10%. Hence, the principal difference between the models lies in the gradient dissipation and Φ terms. At first appearance, the various models appear to have far more similarities than differences. However, as will be seen, each model is quite unique.

Integration Through the Sublayer: Viscous Modifications

At this point, some distinct differences between the equations for the three turbulence quantities, ϵ_d, ℓ, and ω, can be brought to light by studying the model equations when molecular viscosity is added simply by incorporating it into the diffusion terms. The differences are made evident by considering appropriate boundary conditions at a solid boundary.

Boundary conditions suitable for integration through the sublayer have already been developed for the Saffman-Wilcox and Wilcox-Traci models; these boundary conditions reflect effects of surface roughness. The similarity between the various models noted earlier suggests that surface-roughness effects can be represented within dissipation-function and length-scale formulations in as simple a manner as with the Saffman-Wilcox model. Hence, we seek viscous modifications analogous to those devised by Saffman-Wilcox and Wilcox-Traci for rough walls.

Table 2 Coefficients in transformed model equations

Model	c_ω	β^*	β	σ^*	σ	χ
Jones-Launder	1.10	.09	.18	1.0	0.769	2
Ng-Spalding	1.04	.09	.152	1.0	1.0	6
Saffman-Wilcox	.55-.88	.09	.15-.18	0.5	0.5	0
Wilcox-Traci	1.11	.09	.15	0.5	0.5	2

In the Saffman-Wilcox[7] approach, molecular viscosity is introduced in the diffusion terms of the momentum equation and the equations for e and ω. The following surface boundary conditions are then imposed:

$$e=0, \quad \omega=u_\tau^2 S(ku_\tau/\nu)/\alpha^*\nu \quad \text{at } y=0 \tag{22}$$

where u_τ is friction velocity, ν is kinematic viscosity, and S is a universal function of wall roughness, k. Saffman and Wilcox have developed the following correlation between S and ku_τ/ν for fully turbulent flows:

$$ku_\tau/\nu \doteq 50\, S^{-1/2} \tag{23}$$

Therefore, Eqs. (22) can be replaced by

$$e=0, \quad \omega=2500\nu/\alpha^* k^2 \quad \text{at } y=0 \tag{24}$$

Similar boundary conditions have been developed for the Wilcox-Traci[8] model. Note that in developing these boundary conditions, it is essential that the equations admit solutions for arbitrary surface values of ω.

Following the Saffman-Wilcox approach, we add molecular diffusion to the turbulent energy equation for the Jones-Launder and Ng-Spalding models, so that

$$de/dt=\epsilon\{\partial u/\partial y\}^2-\beta^* e\omega+\partial[(\nu+\sigma^*\epsilon)\partial e/\partial y]/\partial y \tag{25}$$

Upon adding molecular diffusion to the Jones-Launder dissipation function equation and the Ng-Spalding length-scale equation and upon transforming to canonical variables (e,ω), we find the following:

Jones-Launder Model

$$\begin{aligned} d\omega^2/dt=&c_\omega\{\partial u/\partial y\}^2\omega-\beta\omega^3+\partial[(\nu+\sigma\epsilon)\partial\omega^2/\partial y]/\partial y \\ &-1/2(\nu+\sigma\epsilon)[(\partial\omega^2/\partial y)/\omega^2-4(\partial e/\partial y)/e]\partial\omega^2/\partial y \\ &+2(\sigma-\sigma^*)(\omega^2/e)\partial[\epsilon\partial e/\partial y]/\partial y \end{aligned} \tag{26}$$

Ng-Spalding Model

$$\begin{aligned} d\omega^2/dt=&c_\omega\{\partial u/\partial y\}^2\omega-\beta\omega^3+\partial[(\nu+\sigma\epsilon)\partial\omega^2/\partial y]/\partial y \\ &-3/2(\nu+\sigma\epsilon)[(\partial\omega^2/\partial y)/\omega^2-(\partial e/\partial y)/e]^2\omega^2 \end{aligned} \tag{27}$$

For simplicity, the Ng-Spalding wall dissipation term has been dropped in Eq. (27); further comment on its effect upon sublayer structure will be given below. A key feature of Eqs. (26) and (27) is the appearance of molecular viscosity in the gradient-dissipation terms. As will be discussed, these *viscous gradient-dissipation terms* strongly affect solution behavior as $y\to 0$.

Our objective is to determine whether the Jones-Launder and Ng-Spalding models have solutions with $e=0$ at $y=0$ and with ω assigned an arbitrary constant value. Assuming the solutions are analytic as $y\to 0$ we seek power series solutions of the form

$$u=u_1 y+\tfrac{1}{2}u_2 y^2+\ldots \tag{28a}$$

$$e=e_1 y+\tfrac{1}{2}e_2 y^2+\ldots \tag{28b}$$

$$\omega=\omega_0+\omega_1 y+\tfrac{1}{2}\omega_2 y^2+\ldots \tag{28c}$$

Neglecting convective terms, we find, to leading order, that for the Jones-Launder, Ng-Spalding, and Saffman-Wilcox models, the turbulent energy equation yields

$$e_2=-\sigma^* e_1^2/\omega_0\nu \tag{29}$$

Results for the Wilcox-Traci model are virtually identical to those for the Saffman-Wilcox model, and are therefore deleted for brevity.

The leading term from the dissipation rate equation for each model is

Jones-Launder Model

$$[2\nu\omega_1+(\sigma-\sigma^*)e_1]\omega_0=0 \tag{30}$$

Ng-Spalding Model

$$-3/2\nu\omega_0^2=0 \tag{31}$$

Saffman-Wilcox Model

$$\omega_2=(\beta\omega_0-\alpha u_1)\omega_0/2\nu-(1+\sigma e_1/\nu\omega_1)\omega_1^2/\omega_0 \tag{32}$$

Inspection of Eqs. (29) and (32) shows that four constants are free in the Saffman-Wilcox model, namely, u_1, e_1, ω_0, and ω_1. The three constants, u_1, e_1, and ω_1 are determined by conditions far from the surface, while ω_0 can assume arbitrary values. However, neither the Jones-Launder model nor the Ng-Spalding model will admit solutions in which ω_0 can be specified arbitrarily. For the Jones-Launder model, Eq. (30) shows that either $\omega=0$ or $2\nu\partial\omega/\partial y=(\sigma^*-\sigma)\partial e/\partial y$ at $y=0$; in either case, there are only three free coefficients. Equation (31) shows that $\omega=0$ at $y=0$ for the Ng-Spalding model. The conclusion that $\omega=0$ at $y=0$ for the Ng-Spalding model still holds when the wall dissipation term is included; the only significant change is that $e\sim y^2$ as $y\to 0$. Thus, without further viscous modifications, neither the Jones-Launder model nor the Ng-Spalding model represents surface-roughness effects in as simple a manner as the Saffman-Wilcox model.

The source of difficulty in the Jones-Launder and Ng-Spalding models is the strongly singular behavior of the *viscous gradient-dissipation terms*, i.e., the portion of the gradient-dissipation terms proportional to ν. These are the most strongly singular terms in the equations and they dominate solution behavior whenever $e\to 0$, which occurs near a solid boundary and also near the boundary-layer edge. In addition to precluding straightforward representation of surface roughness, these singular terms can cause numerical difficulties. The viscous gradient-dissipation terms are only evident when the Ng-Spalding- and Jones-Launder models are written in the canonical variables e and ω. Presumably, similar terms can be introduced in the untransformed ϵ_d and $e\ell$ equations to force complete cancellation of the singular terms after transformation to the canonical form. Nevertheless, this illustrates the fact that devising suitable viscous modifications for the Jones-Launder and Ng-Spalding models is a more complicated task than it is for the Saffman-Wilcox and Wilcox-Traci models.

Note that these comments pertain only to mathematical considerations, and in no way establish whether any of the models accurately predict observed viscous effects on turbulence at low Reynolds number. To make such an

assessment would require computations including complex flows such as low-Reynolds-number boundary layers, transpired and rough-wall boundary layers, and wall jets with pressure gradient. While such a study certainly has merit, the computational effect is great. However, by focusing upon high-Reynolds-number equilibrium boundary layers, an important first step can be made which involves a much more modest computational effort. We thus confine the remainder of this paper to flows for which viscous effects are sufficiently small that the classical law of the wall applies close to the solid boundary.

III. Comparisons for Equilibrium Boundary Layers

The four models are first applied to equilibrium boundary layers. The equilibrium case is of great importance for two critical reasons. First, detailed experimental data are available for such boundary layers, thus permitting definitive tests of the theories. Second, to be of any practical use, two-equation models certainly must perform as well as the much-simpler mixing-length method,[14] the latter being quite accurate for equilibrium boundary layers.

To provide an objective comparison of the various models, all calculations have been performed with the same computer program. Also, starting profiles and boundary conditions are identical for all of the models. The computer program used is an incompressible version of a second-order accurate, implicit boundary-layer program known as EDDYBL.[15] The numerical method embodied in EDDYBL is that developed by Flugge-Lotz and Blottner.[16] The flows considered are listed in Table 3; corresponding experimental data sources are also given.

While the comparison of computed flow properties is of primary interest, an interesting corollary observation has been made. As the study progressed, it was found that the models are not overly sensitive to either boundary-layer-edge boundary conditions or to the starting e and ω, ℓ, or ϵ_d profiles as long as reasonable values are used. With e being defined as $9/4\langle v'^2\rangle$, it is a straightforward task to assign its edge boundary condition and starting profile. At the outset, it was not clear how to prescribe the edge boundary condition and starting profile for a quantity such as ω. However, the length scale, ℓ, is the easiest to work with; enough empirical information is known about ℓ to minimize guesswork when determining edge boundary conditions and starting profiles. Once cast in terms of the length scale, the boundary conditions and starting profiles can readily be transformed to an ϵ_d and ω form compatible with the Jones-Launder, Saffman-Wilcox, and Wilcox-Traci formulations. Since sufficient details of turbulence properties needed to define starting profiles and boundary conditions are often unavailable, the models' insensitivity to boundary conditions and starting profiles is a valuable feature. Thus before presenting results of the computations, we present further details of the boundary conditions and starting profiles used.

Boundary Conditions

Boundary conditions must be specified at the boundary-layer edge and at the solid surface. Surface boundary conditions are analyzed first. Since the inviscid forms of the four models are considered, it is not possible to integrate through the viscous sublayer. Hence, it is necessary to assume that the sublayer has zero thickness and to match to the law of the wall. A singular perturbation expansion of the model equations, valid as $y/\delta \to 0$ where δ is boundary-layer thickness, yields the proper boundary conditions. Such a perturbation expansion solution for the Saffman-Wilcox and Wilcox-Traci models is

$$u/u_\tau = \kappa^{-1}\log u_\tau y/\nu + B, \quad e = u_\tau^2/\alpha^*,$$

$$\omega = u_\tau/\alpha^*\kappa y \quad \text{as} \quad y/\delta \to 0 \tag{33}$$

Table 3 Flows computed in two-equation-model comparisons

Flow	Data sources
Flat plate boundary layer	Karman-Schoenherr[17] skin friction corelation; Klebanoff[18] data; Wieghardt[19] data.
Bradshaw adverse pressure gradient	Bradshaw[20] data; Coles'[19] version of Bradshaw data.
Andersen adverse pressure gradient	Andersen[21] data.
Ludwieg-Tillmann favorable pressure gradient	Ludwieg-Tillmann[19] data; Coles'[19] version of Ludwieg-Tillman data.

The quantity u_τ is the friction velocity, $\kappa = 0.41$ is Karman's constant, $\alpha^* = 3/10$ is the constant in the Saffman-Wilcox and Wilcox-Traci formulations, and B is the constant in the law of the wall. The constant B, which can only be determined by integrating through the sublayer, was assumed to be 5.5 in all computations. The Jones-Launder and Ng-Spalding models give the same expressions for the velocity and turbulent mixing energy. These models yield an expression analogous to the last of Eqs. (33) for their respective second turbulence parameters ϵ_d and ℓ. The boundary conditions on ϵ_d and ℓ can be obtained directly from Eqs. (33) by using the relations between ω, ϵ_d, and ℓ [Eq. (19)]. It is a straightforward procedure to show that the above boundary conditions hold for flows with pressure gradient as well as for constant pressure flows.

Equations (33) must be applied close to the wall, at least closer than $y^+ = u_\tau y/\nu = 20$ and preferably at a y^+ of 10. Applying the conditions closer than a y^+ of 10 makes little difference other than increasing computing time; applying them above $y^+ = 20$ significantly affects the solutions. On first inspection, it may seem inaccurate to apply the boundary

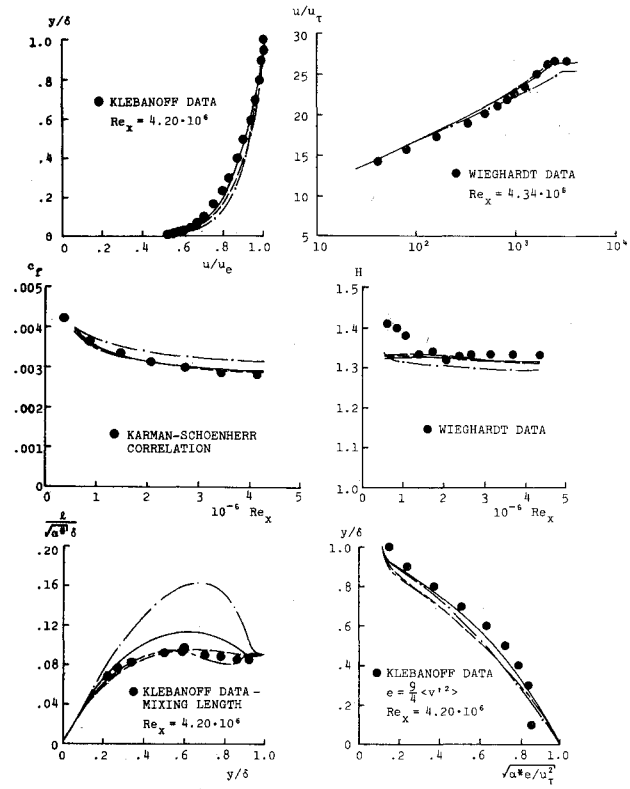

Fig. 1 Comparison of computed and measured flow properties for flat-plate boundary-layer flow; ——Jones-Launder, – – –Ng-Spalding, — · —Saffman-Wilcox, ——Wilcox-Traci. Velocity profiles and c_f and H distributions for the Jones-Launder and Ng-Spalding models are virtually identical.

conditions so close to the wall where, physically, the law of the wall does not hold (i.e., $y^+ \leq 30$). However Eqs. (33) are the rigorous solution to the inviscid model equations as $y/\delta \to 0$. The singular behavior of u and ω results from assuming that the sublayer has negligible thickness. These singularities can be removed by matching to a sublayer solution valid in the limit $u_\tau y/\nu \to \infty$.

Turning now to boundary conditions at $y=\delta$, u must equal the boundary-layer-edge velocity, u_e. Additionally, boundary conditions must be prescribed for the two turbulence parameters in each model. The boundary conditions imposed for each model are as follows:

$$e = .015u_\tau^2/\alpha^*, \quad \ell = .09\sqrt{\alpha^*}\,\delta \quad \text{at } y=\delta \tag{34}$$

A defect-layer perturbation analysis of the Saffman-Wilcox and Wilcox-Traci models[8] helped determine the boundary-layer-edge value of the turbulent mixing energy. The defect-layer analysis shows that a value of e corresponding to $\alpha^* e/u_\tau^2 = .015$ is the largest value consistent with the equations that yields accurate defect-layer velocity profiles. Using smaller values of e makes little difference while $\alpha^* e/u_\tau^2 = .015$ proves easier to handle numerically. We assume that the same value of e is appropriate for all four models. The quantity $\ell/\sqrt{\alpha^*}$ is very similar to the classical mixing length, ℓ_m. A value of $\ell_m/\delta = .09$ at the boundary-layer edge has been empirically found to be appropriate for high Reynolds number boundary layers. As part of the present study, we varied the edge value of $\ell/\sqrt{\alpha^*}\,\delta$ from .06 to .12; all four models showed only slight differences in the numerical solutions resulting from this variation. Hence, as noted above, once realistically chosen boundary conditions are prescribed, excursions from these values have little effect on the solutions to the model equations.

Starting Profiles

Starting profiles can easily be obtained if sufficient information is given at the starting location. By noting that e is $9/4\langle v'^2\rangle$ and by making the eddy viscosity approximation

$$e^{1/2}\ell\,\partial u/\partial y = \langle -u'v'\rangle \tag{35}$$

then u, $\langle v'^2\rangle$ and $\langle -u'v'\rangle$ data completely determine u, e, and ℓ profiles. For both the Andersen adverse pressure gradient and Bradshaw adverse pressure gradient cases, u, $\langle v'^2\rangle$ and $\langle -u'v'\rangle$ data are available so that u, e, and ℓ profiles can be uniquely defined.

Due to the wealth of information on flat plate boundary (FPBL) flow, starting profiles can easily be obtained. Mean velocity profiles are specified using Coles' composite law-of-the-wall/law-of-the-wake profile,[19] i.e.,

$$u/u_\tau = \kappa^{-1}\log u_\tau y/\nu + B + (2\tilde{\pi}/\kappa)\sin^2(\tfrac{1}{2}\pi y/\delta) \tag{36}$$

where $\tilde{\pi}$ is the wake strength. The FPBL $9/4\langle v'^2\rangle$ profile can be approximated by

$$e_{\text{FPBL}} = (u_\tau^2/\alpha^*)\cos^2(\tfrac{1}{2}\pi\, y/\delta) \tag{37}$$

Finally, the high Reynolds number FPBL length scale, ℓ_{FPBL}, empirically has been found to have the following character.

$$\ell_{\text{FPBL}} = \begin{cases} \kappa\sqrt{\alpha^*}\,y, & y \leq .09\,\delta/\kappa \\ .09\sqrt{\alpha^*}\,\delta, & y > .09\,\delta/\kappa \end{cases} \tag{38}$$

Only the mean velocity profile is available for the Ludwieg-Tillmann flow. For simplicity, FPBL profiles for e and ℓ are assumed suitable. The two adverse pressure gradient flows have been recomputed using Eqs. (37) and (38) to determine solution sensitivity to starting profiles. Results are virtually identical to those obtained using profiles inferred from ex-

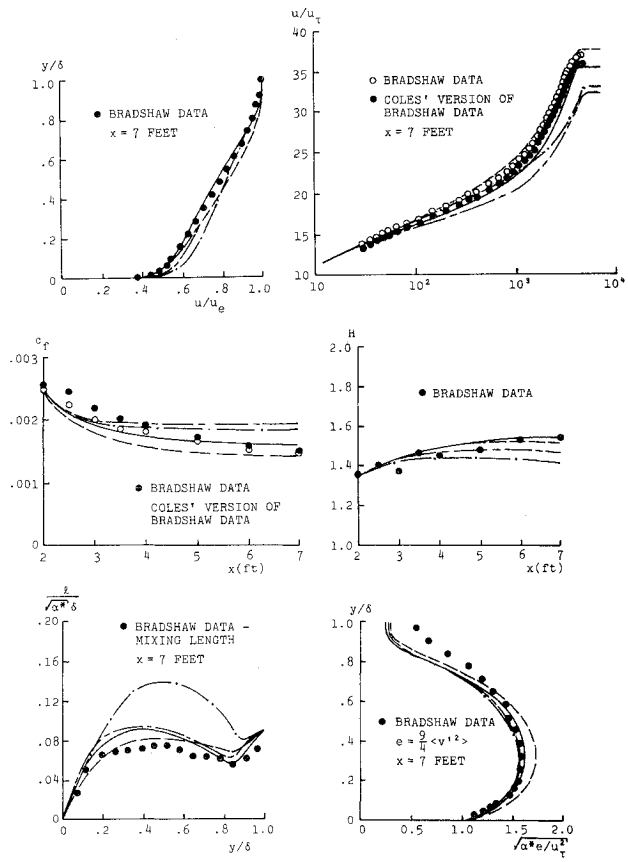

Fig. 2 Comparison of computed and measured flow properties for the Bradshaw adverse pressure gradient flow; ——Jones-Launder, – – –Ng-Spalding, —·—Saffman-Wilcox, ——Wilcox-Traci.

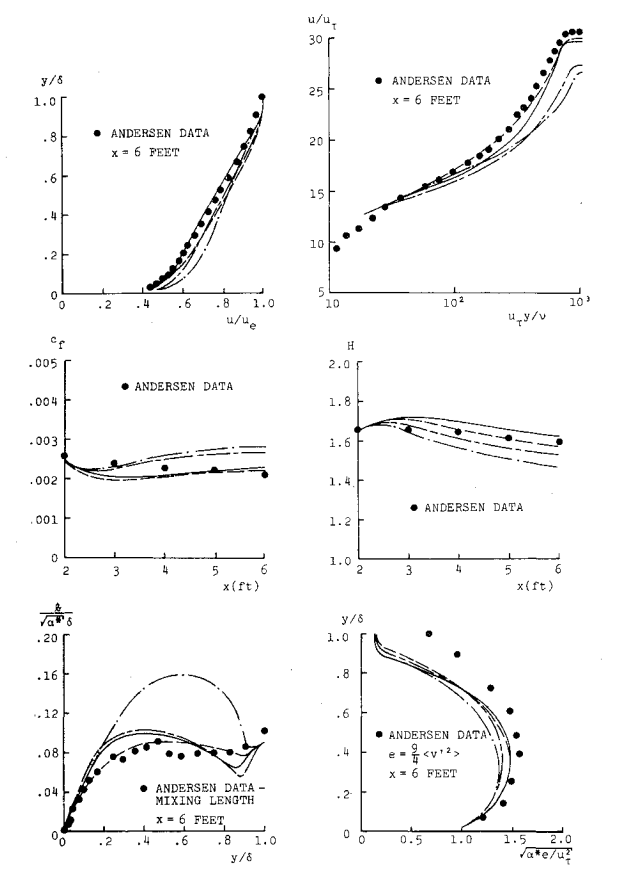

Fig. 3 Comparison of computed and measured flow properties for the Andersen adverse pressure gradient flow;——Jones-Launder, – – –Ng-Spalding, —·—Saffman-Wilcox, ——Wilcox-Traci.

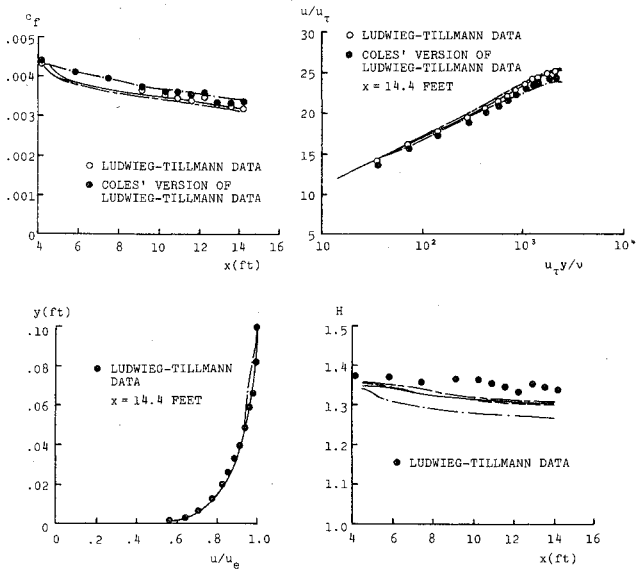

Fig. 4 Comparison and measured flow properties for the Ludwieg-Tillmann favorable pressure gradient flow;——Jones-Launder, – – – Ng-Spalding,—·—Saffman-Wilcox,——Wilcox-Traci.

perimental data. It hence appears that all of the models' solutions are relatively insensitive to reasonable starting profiles.

Results of the Computations

As shown in Fig. 1, all of the models are reasonably accurate for FPBL flow. Computed properties for the Jones-Launder, Ng-Spalding and Wilcox-Traci models are generally within 5% of measurements for the FPBL, while Saffman-Wilcox-model predictions generally differ from corresponding shape factor, H, skin friction, c_f, and velocity and mixing energy profile data by about 10%. Most notably the Saffman-Wilcox model has a length scale profile which has a peak value nearly double that of the Klebanoff mixing-length profile. The Wilcox-Traci model yields a velocity profile in linear (u/u_e vs y/δ) coordinates which agrees most closely with experimental data.

The Ng-Spalding and Wilcox-Traci models yield the closest agreement between computed and measured properties for both adverse pressure gradient flows, whereas the Jones-Launder-model and the Saffman-Wilcox-model predictions differ from the data substantially (Figs. 2 and 3). The Ng-Spalding and Wilcox-Traci model give length-scale profiles closest to the experimental mixing-length profiles for both adverse pressure gradient flows. Correspondingly, other properties of the flows are well represented. Most particularly, note the excellent agreement between experimental and computed velocity profiles in linear coordinates for the Wilcox-Traci model. The Ng-Spalding model's velocity profiles in linear coordinates do not agree nearly as well with the data as do the Wilcox-Traci model's. However, with the exception of the velocity profile in linear coordinates, the Ng-Spalding model yields closest overall agreement to the Andersen data.

The Ludwieg-Tillmann favorable pressure gradient flow is the easiest of the four flows considered (Fig. 4). The Jones-Launder, Ng-Spalding, and Wilcox-Traci models exhibit close agreement with data for every quantity considered. The Saffman-Wilcox model yields good agreement for the skin friction and velocity profiles in sublayer coordinates; the model exhibits larger discrepancies for shape factor and the velocity profile in linear coordinates. The Saffman-Wilcox-model velocity profile in linear coordinates displays an inflection in the defect layer, typical of Saffman-Wilcox-model solutions.[13]

Inspection of the various e profiles (Fig. 1-3) shows that all of the models accurately reproduce the $9/4\langle v'^2\rangle$ data. However, the various ℓ profiles show considerable differences. It hence appears that accuracy of a two-equation model is controlled by the accuracy with which the turbulent length scale can be computed.

Of the four flows, the models do poorest on the Andersen flow. This is not surprising as the Andersen flow has a relatively low Reynolds number ($U_\infty/\nu = 1.8\cdot 10^5/\text{ft}$) and, without suitable viscous corrections, the models are realistically only applicable at high Reynolds numbers. This is best exemplified in Fig. 3. The Ng-Spalding and Wilcox-Traci models stray from skin friction data early in the computation. However, agreement is much better by the end of the computation where the boundary layer finally approaches a well-developed turbulent state.

In summary, the Ng-Spalding and Wilcox-Traci models yield results in much closer agreement with the data than do the Jones-Launder and Saffman-Wilcox models. Furthermore, the Wilcox-Traci-model's velocity profiles in linear coordinates are in close accord with the data and consistently closer than any of the other models'. In addition, discrepancies between computed and measured flow properties are generally less than 10% for the Wilcox-Traci and Ng-Spalding models, a level of accuracy comparable to that of mixing-length theory. Hence, these two models are as accurate as mixing-length for equilibrium boundary layers. However, this in itself provides insufficient motivation for using two-equation models rather than mixing-length theory. Two-equation models are much more complicated than mixing-length theory and their use is sometimes attended by nontrivial increases in computing time. A wider range of applicability than that of the simpler mixing-length theory must provide the motivation for using a two-equation model. The next section addresses an advanced application which gives an example of this extended range.

IV. Comparison for a Flow with Curved Streamlines

As an arduous test of two-equation models, constant-pressure flow over a convex surface composed the second round of numerical applications. Streamline curvature has a profound effect on turbulent flows which is generally not contained in classical turbulence theories. The mixing-length approach, for example, must be modified *empirically* to obtain accurate predictions for flow over curved surfaces.[22] The two-equation-model theory is also suspect as shown in the turbulent vortex computations of a) Baldwin and Chigier[23] who used the Jones-Launder model and b) Govindaraju[24] who used an early version of the Saffman-Wilcox model. As will be shown in this section, two-equation models require curvature modifications. However, in contrast to mixing-length theory, the needed modifications can be devised in a nonempirical manner.

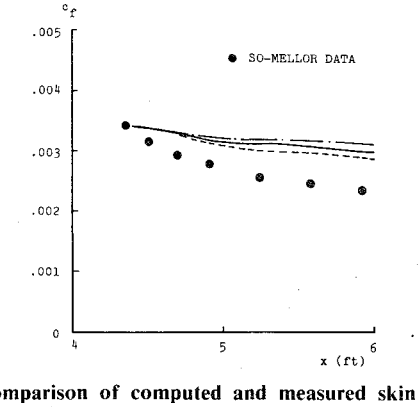

Fig. 5 Comparison of computed and measured skin friction for flow over a curved surface; – – – Jones-Launder/Ng-Spalding,—·—Saffman-Wilcox, ——Wilcox-Traci.

It is unnecessary to look further than the comparison of computed and measured[25] skin friction shown in Fig. 5 to see that none of the models predicts the strong stabilizing effect of the convex wall. This is not surprising since, assuming e and ω are scalar quantities, the curvature affects only the production terms, i.e. $(\partial u/\partial y)$ is replaced by $(\partial u/\partial y - u/R)$, where R is the radius of curvature of the wall. As shown in Fig. 5, this modification is insufficient to account for the large observed effect of curvature.

However, these poor results stem from an erroneous assumption rather than from a failure of two-equation models. We have mistakenly treated the turbulent-mixing-energy equation as a scalar equation. Because the mixing energy is proportional to $\langle v'^2 \rangle$ and because $\langle v'^2 \rangle$ is strongly affected by curvature, assuming that the turbulent mixing energy is a scalar quantity is a physically unrealistic hypothesis. The manner in which $\langle v'^2 \rangle$ is altered by curvature can be seen by examining the exact rms equation for $\langle v'^2 \rangle$, viz,

$$d\langle v'^2 \rangle/dt = -2\langle -u'v' \rangle u/R + \text{other terms} \qquad (39)$$

The first term on the right-hand side of Eq, (39) originates from the centrifugal acceleration term which appears when the vertical momentum equation is written in curvilinear surface-fixed coordinates. Introducing $e = 9/4\langle v'^2 \rangle$ and approximating $\langle -u'v' \rangle \doteq \epsilon \partial u/\partial y$, Eq. (39) becomes

$$de/dt = -9/2(u/R)\epsilon\ \partial u/\partial y + \text{other terms} \qquad (40)$$

Hence, for flow over a curved surface, the turbulent mixing energy equation must be written as

$$de/dt = P - \beta^* \omega e - 9/2(u/R)\epsilon\ \partial u/\partial y + \partial[\sigma^* \epsilon\ \partial e/\partial y]/\partial y \qquad (41)$$

where $P = \alpha^* |\partial u/\partial y - u/R| e$ for the Saffman-Wilcox and Wilcox-Traci models and $P = \epsilon(\partial u/\partial y - u/R)^2$ for the Jones-Launder and Ng-Spalding models.

In a detailed study of streamline curvature effects based on the Wilcox-Traci model, Wilcox and Chambers[26] have shown that no curvature correction term appears in the dissipation-rate equation. This implies that ω is unaltered by curvature and is indeed a scalar quantity. Now, if ω is a scalar, then Eq. (19) implies that ϵ_d and ℓ are not. Hence, not only do curvature modifications appear in the e equations for the Jones-Launder and Ng-Spalding models, but similar terms must also appear in the ϵ_d and $e\ell$ equations. Curvature correction terms for the ϵ_d and $e\ell$ equations can be derived by noting that

$$d\epsilon_d/dt = c_\mu[\omega(de/dt) + \tfrac{1}{2}(d\omega^2/dt)e/\omega]$$

$$= -9/2(\epsilon_d/e)(u/R)\epsilon\partial u/\partial y + \ldots \qquad (42)$$

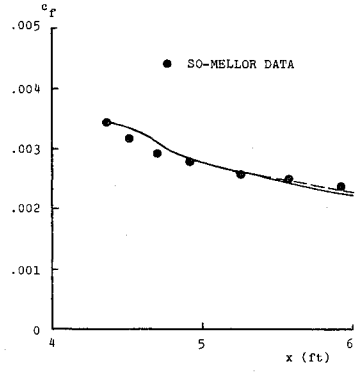

Fig. 6 Comparison of computed and measured skin friction for flow over a curved surface; – – – Jones-Launder/Ng-Spalding, ——Wilcox-Traci. Computations performed using curvature modifications.

and

$$d(e\ell)/dt = [3/2\ell(de/dt) - \tfrac{1}{2}\ell^3(d\omega^2/dt)]$$

$$= -27/4(u/R)\ell\epsilon\partial u/\partial y + \ldots \qquad (43)$$

Therefore, we propose the following modified equations for the Jones-Launder and Ng-Spalding models.

Jones-Launder Model

$$d\epsilon_d/dt = c_1(\epsilon_d/e)\epsilon(\partial u/\partial y - u/R)^2$$

$$-c_2\epsilon_d^2/e - 9/2(\epsilon_d/e)(u/R)\epsilon\ \partial u/\partial y + \partial[(\epsilon/\sigma_\epsilon)\partial\epsilon_d/\partial y]/\partial y \qquad (44)$$

Ng-Spalding Model

$$d(e\ell)/dt = c_p\ell\epsilon(\partial u/\partial y - u/R)^2 - [c_m + c_w(\ell/y)^6]e^{3/2}$$

$$-27/4(u/R)\ell\epsilon\partial u/\partial y + \partial[(\epsilon/\sigma_z)\partial(e\ell)/\partial y]/\partial y \qquad (45)$$

As noted above, the only alteration to the Saffman-Wilcox and Wilcox-Traci ω^2 equations is in the production terms where $|\partial u/\partial y|$ is replaced by $|\partial u/\partial y - u/R|$.

With these curvature modifications, the convex-surface flow was recomputed using the Jones-Launder, Ng-Spalding, and Wilcox-Traci models. Figure 6 compares computed and measured skin friction. For all three models, computed c_f is within 5% of measured values. Hence, with proper interpretation of the turbulence properties, two-equation models can be used to accurately predict effects of streamline curvature on turbulent boundary layers.

V. Discussion

Results of the streamline curvature computations and the algebraic analysis of model-equation behavior in the sublayer support the notion that e and ω are "canonical" turbulence parameters for two-equation models. First, the invariance of ω in a curved coordinate system greatly simplifies analysis of streamline curvature effects on turbulent boundary layers. Second, unwitting introduction of strongly singular viscous-gradient-dissipation terms in the sublayer can be avoided by working directly with ω rather than with ϵ_d or ℓ.

The equilibrium boundary-layer applications of Sec. III show that the Wilcox-Traci and Ng-Spalding models yield results in much closer agreement with the experimental data than do the Jones-Launder and Saffman-Wilcox models. Furthermore, the Wilcox-Traci model's velocity profiles in linear coordinates are in very close accord with data and consistently closer than any of the other models. It is reasonable to claim that for incompressible flows, the Ng-Spalding and the Wilcox-Traci two-equation models are as accurate as mixing-length theory where mixing length applies. This by itself is not justification for the continued development of these sophisticated models. However, it must be the case that the models do as well as mixing length if two-equation models are to become believable predictive tools for a larger class of flows than mixing-length models can handle. As indicated by the computation of flow over a convex wall, the two-equation models do have a wider range of applicability. This, in conjunction with their accuracy for equilibrium boundary layers, provides sufficient motivation for more widespread use of two-equation models.

Acknowledgment

This research was sponsored by NASA Ames Research Center under Contracts NAS2-8884 and NAS2-9135.

References

[1]Kolmogorov, A. N., "Equations of Turbulent Motion of an Incompressible Fluid," *Izvestia Academy of Sciences, USSR; Physics*, Vol. 6, Nos. 1 and 2, 1942, pp. 56-58.

[2]Saffman, P. G., "A Model for Inhomogeneous Turbulent Flow," *Proceedings of the Royal Society London, A*, Vol. 317, 1970, pp. 417-433.

[3]Wilcox, D. D. and Alber, I. E., "A Turbulence Model for High Speed Flows," *Proceedings of the 1972 Heat Transfer and Fluid Mechanics Institute*, June 14-16, 1972, pp. 231-252, Stanford Univ. Press, Stanford, Calif.

[4]Gibson, M. M. and Spalding, D. B., "A Two-Equation Model of Turbulence Applied to the Prediction of Heat and Mass Transfer in Wall Boundary Layers," Paper No. 72-HT-15, AIChE-ASME Heat Transfer Conference, Denver, Colo., Aug. 6-9, 1972.

[5]Jones, W. P. and Launder, B. E., "The Prediction of Laminarization with a Two-Equation Model of Turbulence," *International Journal of Heat and Mass Transfer*, Vol. 15, 1972, pp. 301-314.

[6]Ng, K. H. and Spalding, D. B., "Turbulence Model for Boundary Layers near Walls," *The Physics of Fluids*, Vol. 15, Jan. 1972, pp. 20-30.

[7]Saffman, P. G. and Wilcox, D. C., "Turbulence-Model Predictions for Turbulent Boundary Layers," *AIAA Journal*, Vol. 12, April 1974, pp. 541-546.

[8]Wilcox, D. C. and Traci, R. M., "A Complete Model of Turbulence," AIAA Paper 76-351, San Diego, Calif., 1976.

[9]Wilcox, D. C., "Numerical Study of Separated Turbulent Flows," *AIAA Journal*, Vol. 13, May 1975, pp. 555-556.

[10]Wilcox, D. C., "Turbulence-Model Transition Predictions," *AIAA Journal*, Vol. 13, Feb. 1975, pp. 241-243.

[11]Launder, B. E. and Spalding, D. B., *Mathematical Models of Turbulence*, Academic Press, London, 1972.

[12]Mellor, G. L. and Herring, H. J., "A Survey of Mean Turbulent Field Closure Models," *AIAA Journal*, Vol. 11, May 1973, pp. 590-599.

[13]Wilcox, D. C. and Chambers, T. L., "Streamline Curvature Effects on Turbulent Boundary Layers," DCW Industries, Studio City, Calif., Report DCW-R-04-01, Feb. 1975.

[14]Cebeci, T. and Smith, A. M. O., "A Finite-Difference Solution of the Incompressible Turbulent Boundary-Layer Equations by an Eddy-Viscosity Concept," *Proceedings: Computation of Turbulent Boundary Layers—1968 AFOSR-IFP-Stanford Conference*, Vol. I, Method, Predictions, Evaluation and Flow Structure, Dept. Mech. Engr., Stanford University, Calif., 1968.

[15]Wilcox, D. C., "User's Guide for the EDDYBL Computer Program," DCW Industries, Studio City, Calif., Report DCW-R-14-02, Nov. 1976.

[16]Flugge-Lotz, I. and Blottner, F. G., "Computation of the Compressible Laminar Boundary-Layer Flow Including Displacement-Thickness Interaction Using Finite-Difference Methods," AFOSR 2206, 1962.

[17]von Karman, T., "Turbulence and Skin Friction," *Journal of the Aeronautical Sciences*, Vol. 1, Jan. 1934, pp. 1-20.

[18]Klebanoff, P. S., "Characteristics of Turbulence in a Boundary Layer with Zero Pressure Gradient," NACA 1247, 1955.

[19]Coles, D. E. and Hirst, E. A., *Proceedings: Computation of Turbulent Boundary Layers—1968 AFOSR-IFP-Stanford Conference*, Vol. II, Compiled Data, Dept. Mech. Engr., Stanford University, Calif.

[20]Bradshaw, P., "The Response of a Constant-Pressure Turbulent Boundary Layer to the Sudden Application of an Adverse Pressure Gradient," ARC R&M 3575, 1969.

[21]Andersen, P. S., Kays, W. M., and Moffat, R. J., "The Turbulent Boundary Layer on a Porous Plate: An Experimental Study of the Fluid Mechanics for Adverse Free-Stream Pressure Gradients," Dept. Mech. Engr., Stanford University, Calif., Rept. No. HMT-15, 1972.

[22]Eide, S. A. and Johnston, J. P., "Prediction of the Effects of Longitude Wall Curvature and System Rotation on Turbulent Boundary Layers," Dept. Mech. Engr., Stanford University, Calif., Rept. No. PD-19, 1974.

[23]Baldwin, B. S., Chigier, N. A. and Sheaffer, Y. S., "Decay of Far Flow Field in Trailing Vortices," NASA TN D-7568, 1974.

[24]Govindaraju, S. P., "A Study of Some Turbulent Flows Using a Model for Inhomogeneous Turbulence," Ph.D. Cal. Tech., Pasadena, Calif., 1970.

[25]So, R. M. C. and Mellor, G. L., "An Experimental Investigation of Turbulent Boundary Layers Along Curved Surfaces," NASA CR-1940, 1972.

[26]Wilcox, D. C. and Chambers, T. L., "Streamline Curvature Effects on Turbulent Boundary Layers," AIAA Paper 76-353, San Diego, Calif., 1976; submitted to *AIAA Journal*.